1991

Current Distribution in a HORIZON® Lead-Acid Battery during Discharge

Z. Mao
Texas A & M University - College Station

Ralph E. White
University of South Carolina - Columbia, white@cec.sc.edu

B. Jay

Publication Info

Journal of the Electrochemical Society, 1991, pages 1615-1620.

The displacement of this horizontal line also reflects the effect of curvature on the system behavior. Since in the rectilinear case the voltage drop is proportional to the separation distance between the two interfaces, but is only proportional to the natural logarithm of that distance in the cylindrical cases, curvature results in a reduction of polarization. The value of the asymptote for the rectilinear porous electrode case is $\log [\sigma\kappa/(\sigma + \kappa)^2]$.

Consider a third situation: Suppose δ is large, but $\gamma = 0$. The reaction zone is confined only to a thin region near the electrode/separator interface. In this case, Eq. [23] becomes

$$j^* \rightarrow \left(\frac{2 - \omega}{2}\sqrt{\delta}\right)\left[B_1 \frac{e^{\zeta}}{\sqrt{2\pi\zeta}} + B_2 \sqrt{\frac{\pi}{2\zeta}} e^{-\zeta}\right] \quad [33]$$

Since as δ becomes large

$$B_1 \rightarrow 0 \quad [34]$$

and

$$B_2 \rightarrow \sqrt{\frac{2}{\pi\omega(1 - \omega)}}\, \delta^{1/4} e^{\zeta_1} \left(\frac{\sigma}{\sigma + \kappa}\right) \quad [35]$$

rearrangement of Eq. [33] leads to

$$\frac{[\phi_2|_{\xi=0} - \phi_1|_{\xi=1}]}{(r_o - r_i) i_2|_{\xi=0} (1/\sigma + 1/\kappa)} = \frac{1}{\sqrt{\delta}} \quad [36]$$

which predicts a -0.5 slope on a logarithmic plot of $\Delta\Phi$ against δ. On account of the shallow penetration depth under these conditions, curvature does not impose any significant effect on the polarization behavior. However, Fig. 5 shows that this asymptote is approached sooner at lower values of δ for smaller values of ω. This is because it takes more severe conditions to shift the reaction zone inward when the curvature is high.

Figures 4 and 5 can be very useful for evaluating initial polarization in different systems. From the characteristic δ, γ, and ω values listed in Table I, it is expected that the initial polarization loss in the larger alkaline cells would be greater.

Conclusions

A secondary current distribution model is presented to analyze the reaction distribution at an annular porous electrode. The model is applied to assess the extent of initial polarization in the alkaline cells and provide an estimation of the system behavior without mass-transfer considerations. It is found that because of the greater thickness of the MnO_2 electrode used in the larger capacity cells, unequivalent polarization characteristics are embedded in these cells. Our next paper will examine the additional impact of concentration variations on the cell behavior.

The present model also provides further insights into curvature effects on the performance behavior of cylindrical porous electrodes. If the basis of comparison is taken at the electrode/separator interface at the inner radius of the annular domain, then curvature is shown to reduce the polarization at the electrode.

Manuscript submitted July 9, 1990; revised manuscript received Jan. 4, 1991.

Duracell, Incorporated, assisted in meeting the publication costs of this article.

REFERENCES

1. C. Y. Mak, H. Y. Cheh, G. S. Kelsey, and P. Chalilpoyil, *This Journal*, **138**, 1607 (1991).
2. J. Newman and W. Tiedemann, *AIChE J.*, **21**, 25 (1975).
3. R. E. Meredith and C. W. Tobias, in "Advances in Electrochemistry and Electrochemical Engineering," Vol. 2, C. W. Tobias, Editor, p. 15, Wiley Interscience, New York (1962).
4. R. Pollard and J. S. Newman, *This Journal*, **128**, 491 (1981).
5. M. Abramowitz and I. A. Stegun, "Handbook of Mathematical Functions," 9th ed., p. 374, Dover Publications, Inc., New York (1970).

Current Distribution in a HORIZON® Lead-Acid Battery during Discharge

Z. Mao* and R. E. White*

Center for Electrochemical Engineering, Department of Chemical Engineering, Texas A&M University, College Station, Texas 77843-3122

B. Jay*

Electrosource, Incorporated, Austin, Texas 78744

ABSTRACT

A simple mathematical model is presented and used to analyze the potential and current distributions in a HORIZON® sealed lead-acid battery. It was found that an increase in the thickness of an electrode would not enhance the discharge rate of that electrode; instead, it causes the transfer current distribution to be less uniform in the electrode. Also, the ohmic drop across the separator would decrease with a decrease in the thickness of the separator more rapidly when the thickness is small than when it is large. In addition, it was found that efficient high-capacity, high-rate electrodes must consider the electrode reaction kinetics because of the high sensitivity of transfer current distribution to the reaction kinetics.

The use of coextruded lead-composite wire as a new material for lead-acid battery grids has many advantages over conventional cast lead grids (1). For example, coextruded lead-composite wire achieves high tensile strength and conductivity with light weight. Research into such materials for use in lead-acid batteries by Tracor, Incorporated, has led to an innovative sealed lead-acid battery (SLAB) design by Electrosource, Incorporated, known as the HORIZON® design. This battery design features the use of coextruded grid material, cureless paste, horizontal plates, and a bipolar/monopolar hybrid architecture (1). However, as the battery departs from conventional SLAB design practice in many important areas, the grid design needs to be further optimized. To achieve such optimization, the

* Electrochemical Society Active Member.

current and potential distributions in a HORIZON® battery for several grid designs have been analyzed by using the simple mathematical model presented here. Conclusions obtained, however, can be applied to the general practice of battery grid design.

Model Equations

Mathematical models have been used extensively to predict the performance of lead-acid batteries and to aid the design of such batteries. One-dimensional models (2-4) have been widely used to investigate the effects of acid concentration, electrode porosity, and potentials in the solid and the electrolyte phases during charge and discharge. These studies have significantly enhanced our understanding of the phenomena in such batteries. Tiedemann and co-workers (5, 6) and Sunu and Burrows (7, 8) used an equivalent resistor network approach to investigate the potential and current density distributions on electrode plates. Their work has led to significant improvements in grid design. Recently, Dimpault-Darcy and co-workers (9) expanded their one-dimensional model to two dimensions and found that changes in acid concentration and current density are profound, primarily in the direction perpendicular to the electrode surface. Their results may be due in part to the assumption that the H_2SO_4 concentration does not change at the interface between the porous electrode and the electrolyte. In this work, efforts were made to investigate the effects of grid design, plate separation, and geometry on the potential and current density distributions in Horizon® electrodes. Battery performance is best when concentration polarization is lowest. However, performance also depends strongly on grid design and separator and plate thickness. This work investigates sensitivity of maximum performance on those battery design parameters described above. Therefore, mass-transport processes during the discharge are not explicitly considered. The model region includes the cathode, separator, and the anode in two dimensions as shown in Fig. 1. A finite element technique [IMSL's PDE/PROTRAN, Ref. (10)] was used in the computation because of the relative ease with which this technique can be used to treat curved boundaries.

Based on the macro homogeneous approach (11), both the lead dioxide and lead electrodes are assumed to consist of a homogeneous mixture of solid and liquid phases. Since the conductivities of lead dioxide and lead are many orders of magnitude greater than that of the electrolyte, potential variations in the solid phase of both the cathode and the anode are assumed to be negligible in comparison with those in the electrolyte. That is, the potentials in the solid phases are assumed to be constant, equal to given values. The potential in the electrolytes varies according to Ohm's law

$$\sigma_e \frac{\partial \phi}{\partial x}\mathbf{i} + \sigma_e \frac{\partial \phi}{\partial y}\mathbf{j} = -I_{xy} \qquad [1]$$

where σ_e represents the effective conductivity of the electrolyte, and $\mathbf{i}$ and $\mathbf{j}$ are unit vectors in the x and y directions, respectively. I_{xy} represents the local current density at (x, y) in the electrolyte.

Since electrical charge is neither produced nor consumed in the separator, the divergence of the current density, I_{xy} in this region is equal to zero, yielding the equation

$$\sigma_s \frac{\partial^2 \phi}{\partial x^2} + \sigma_s \frac{\partial^2 \phi}{\partial y^2} = 0 \quad \text{in the separator} \qquad [2]$$

When the cell is discharged, electrons are removed from the anode and supplied to the cathode. Negative electrical charge must therefore be transferred from the electrolyte to the solid phase within the anode through the anodic reaction

$$Pb + SO_4^{2-} - 2e^- \rightarrow PbSO_4 \qquad [3]$$

The opposite process occurs in the cathode through the cathodic reaction

$$PbO_2 + SO_4^{2-} + 4H^+ + 2e^- \rightarrow PbSO_4 + 2H_2O \qquad [4]$$

Therefore, the divergence of the current density in the electrolyte is equal in magnitude but opposite in sign to the transfer current per unit volume in both the cathode and the anode, which results in the following equations

$$\sigma_c \frac{\partial^2 \phi}{\partial x^2} + \sigma_c \frac{\partial^2 \phi}{\partial y^2} = -a_c i_c \quad \text{in the cathode} \qquad [5]$$

$$\sigma_a \frac{\partial^2 \phi}{\partial x^2} + \sigma_a \frac{\partial^2 \phi}{\partial y^2} = -a_a i_a \quad \text{in the anode} \qquad [6]$$

where σ_i represents the effective conductivity of the electrolyte in region i, which is calculated from the electrolyte conductivity, σ, multiplied by a correction term using the equation

$$\sigma_i = \sigma \epsilon_i^{1.5} \qquad [7]$$

where ϵ_i is the porosity of region i (2). The constants a_a and a_c in Eq. [4] and [6] are the specific surface area per unit volume of the anode and the cathode, respectively. The symbols, i_a and i_c, represent the anodic and cathodic current densities due to reactions [3] and [4], respectively, which are expressed by the Butler-Volmer equation

$$i_a = i_{a,o}\left\{\exp\left[\frac{\alpha_a F}{RT}(E_a - \phi - E_{a,o})\right] - \exp\left[-\frac{\alpha_c F}{RT}(E_a - \phi - E_{a,o})\right]\right\} \qquad [8]$$

$$i_c = i_{c,o}\left\{\exp\left[\frac{\beta_a F}{RT}(E_c - \phi - E_{a,o})\right] - \exp\left[-\frac{\beta_c F}{RT}(E_c - \phi - E_{c,o})\right]\right\} \qquad [9]$$

where α_i and β_i ($i = a, c$) are the transfer coefficients for the reactions at the anode and the cathode. E_a and E_c are the anode and cathode potentials, respectively, and $E_{a,o}$ and $E_{c,o}$ are the open-circuit potentials of the anode and the cathode with respect to a reference electrode. If the anode is chosen as the reference electrode, $E_{a,o}$ is equal to zero, and $E_{c,o}$ is equal to the open-circuit cell voltage (OCV). The exchange current densities of the anode and cathode reactions are $i_{a,o}$ and $i_{c,o}$. $E_c - E_a$ represents the cell voltage.

Figure 1 presents a schematic cross section of a pair of plates containing four grid wires. The model domain is the area surrounded by the dashed lines of Fig. 1. The boundary conditions for this domain are given by the following

$$-\sigma_x \frac{\partial \phi}{\partial x} n_x - \sigma_y \frac{\partial \phi}{\partial y} n_y = i_n \qquad [10]$$

where i_n is a current density in the direction normal to the boundaries, and n_x and n_y are the x and y components of a

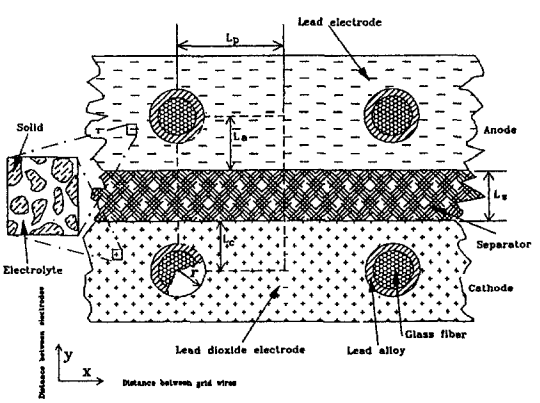

Fig. 1. A schematic view of a cross-sectional area containing four grid wires of the battery.

unit vector outward normal to the boundary surface. The current densities were set to zero for all the boundaries due to symmetry and the assumption that no reaction occurs on wire surfaces. For the inner boundaries, that is, the interfaces between the separator and the cathode or the anode, continuity in the current density is required.

Since the grid wire sheath material (lead alloy) is highly conductive, sheet thickness would not be expected to strongly affect potential within it. Also, the effect of wire length on electric field distribution between the two plates is negligible because the distance between the positive and negative plates is much smaller than the wire length and the grid sheath material is highly conductive. The potential distribution within the model region sets limits on the battery performance. The nonconductive grid core material does not affect current distribution. Therefore, the variables of interest are the wire radius (r), the distance between two neighboring wires ($2Lp$), and the thicknesses of the cathode ($2Lc$), the anode ($2La$), and the separator (Ls).

The PDE/PROTRAN package by IMSL, Incorporated, (10) was used to solve Eq. [2], [5], and [6], subject to the boundary conditions (Eq. [10]). This computational software, based on finite element techniques, provides simple procedures to solve systems of linear or nonlinear two-dimensional differential equations. First, the model region is divided roughly into a few triangles by specifying the location of each individual triangle. The software automatically subdivides those initial triangles into a total number of triangles specified to obtain a desired solution accuracy (see Fig. 2). The governing equations and boundary conditions must be formulated in a form required by the software, but such formulation is quite simple. The fixed parameters for the simulation are given in Table I.

Results and Discussion

Figure 3 represents a typical potential profile (a), the current flow pattern (b), and the corresponding transfer current distribution (c) at a cell voltage 0.1 V lower than the open-circuit cell voltage. The potential in the electrolyte increases significantly from the cathode to the anode (y direction), but it changes only slightly in the x direction. Consequently, the current flows almost vertically through the separator from the anode to the cathode in the cell. As the transfer current adds to the current, the magnitude of the current density increases from the center to the front side of the electrodes, and becomes constant in the separator where electrical charge is neither produced nor consumed (the length of arrows represents the magnitude of the current density). Although both current density and potential distributions are quite uniform, Fig. 3c indicates that the transfer current distribution is highly nonuniform within each electrode. The transfer current is higher along the front sides of the electrodes than it is at the electrode center. That is, the active materials are consumed faster toward the front side of the electrodes. As a result, the active materials at the center of the electrodes would not be fully utilized if passage of the current is blocked by the reaction product in the front side of the electrodes. This nonuniform transfer current density distribution is due to the nonuniform driving potentials, $(E_c - \phi - E_{c,o})$ for the cathode, and $(E_a - \phi - E_{a,o})$ for the anode.

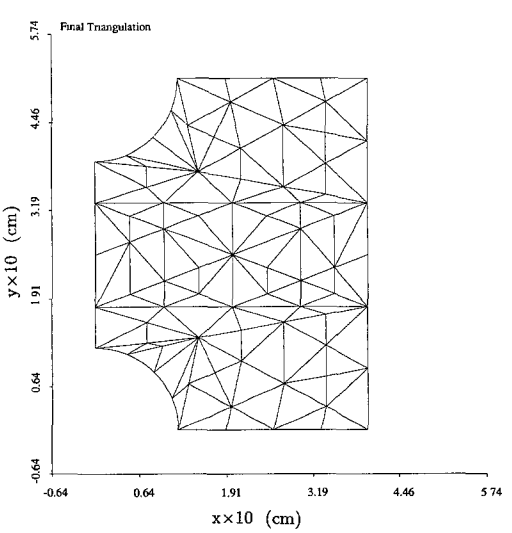

Fig. 2. An example of the division of the model region into a given number of triangles or elements.

Table I. Fixed parameters.

k	α_k	β_k	$i_{k,o}$ (A/cm^2)[a]	ϵ_k
a	1.0	1.0	3.404×10^{-3}	0.61
c	1.0	1.0	2.849×10^{-3}	0.55
s				0.65

T = 25°C, σ = 0.79 S/cm.[b]

[a] From Ref. (3).
[b] The conductivity of 5M H_2SO_4 solution at 25°C (13).

To evaluate the effects of the variables (r, Ls, La, Lp, and Lc) on the potential distribution and the current density distribution, uniformity in the transfer current distribution (Uni) and the total current (I) for a given cell voltage were used as criteria. The term Uni is defined as

$$Uni = \frac{2(I_f - I_b)}{I_f + I_b} \quad [11]$$

where I_f and I_b represent the total transfer current along the front side and the center of the cathode, respectively. The minimum value of Uni is zero, representing perfectly uniform transfer current distribution. The maximum value of 2 for Uni corresponds to the situation in which charge transfer occurs only on the front side of the electrode. The total electrode current was calculated by applying the trapezoidal rule to Eq. [12]

$$I = -\left[\int_0^r \left(\int_{\sqrt{r^2-y^2}}^{Lp} a_c i_c dx\right) dy + \int_r^{Lc}\int_0^{Lp} a_c i_c dx dy\right] \quad [12]$$

where the minus sign before the bracket was used to make the total current positive since the transfer current in the cathode is negative as defined by Eq. [9].

Figures 4a and b represent the effect of cathode thickness on the total current at different cell voltages and on the transfer current distribution, respectively. An increase in the cathode thickness does not produce a corresponding increase in the discharge rate; instead, it causes the transfer current distribution to be less uniform. While it may be inferred that the capacity of an electrode may be increased by making it thicker, its discharge rate cannot be increased by the same means. When the cell is discharged at a high rate, the transfer current distribution becomes less uniform as shown in Fig. 4b, which indicates that utilization of the active material will decrease with an increase in discharge rate. Therefore, to design a high-rate discharge battery with high utilization of active materials, a thin large-surface-area electrode is essential.

If separator thickness is reduced, the ohmic drop across the separator would be expected to decrease correspondingly. Figure 5a shows that at a given cell voltage the current increases with a decrease in separator thickness. It is desirable to plot the product of the total current and the separator thickness ($I \times Ls$) against Ls to indicate the effect of the separator thickness, because the separator resistance is proportional to its thickness and ILs is an indirect measure of the ohmic drop across the separator. As shown in Fig. 5c, the relationship between $I \times Ls$ and Ls is not linear; $I \times Ls$ decreases with a decrease in Ls more rapidly when Ls is small than when Ls is large. Therefore, the separator should be designed as thin as possible. The current distribution becomes less uniform when separator thickness is reduced (see Fig. 5b) because the discharge rate is thus increased.

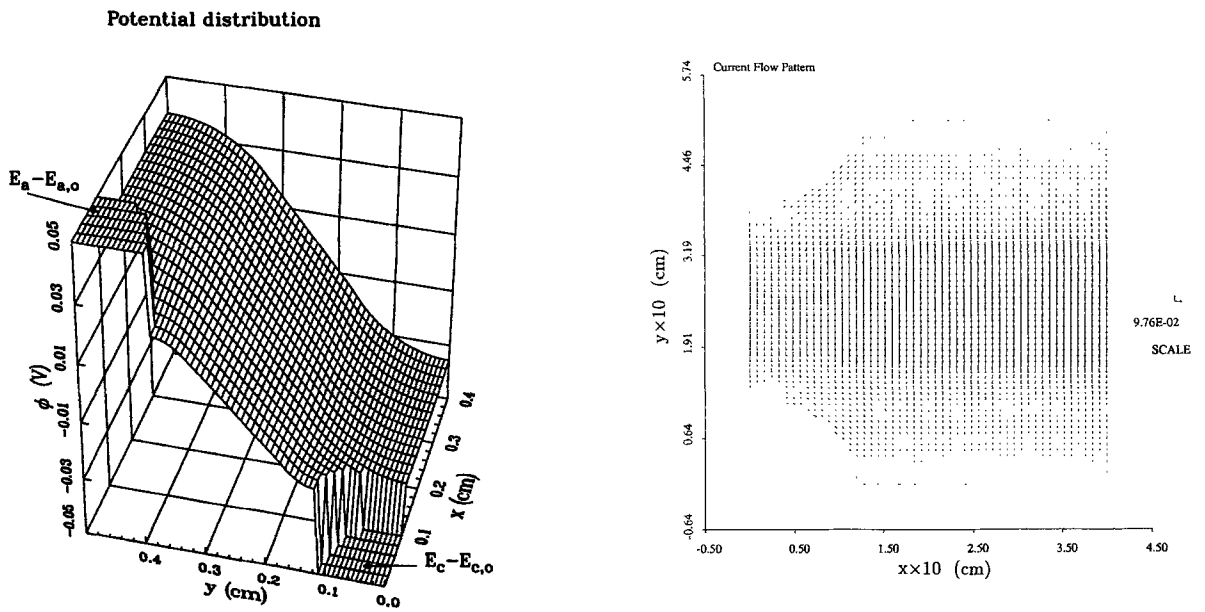

Fig. 3. A typical predicted potential distribution (a, top left), a current flow pattern (b, top right), and the corresponding transfer current distribution (c, left). La = 0.18 cm, Lc = 0.18 cm, Ls = 0.15 cm, Lp = 0.4 cm, r = 0.12 cm, OCV − (E_c − E_a) = 0.1 V.

Since the transfer current distribution along the electrode (in x direction as specified in Fig. 1) is quite uniform, as shown in Fig. 3, an increase in the distance between grid wires (Lp) would increase the total current proportionally. Figure 6 shows an almost linear relationship between the total current and the wire pitch. Figure 6 also shows that

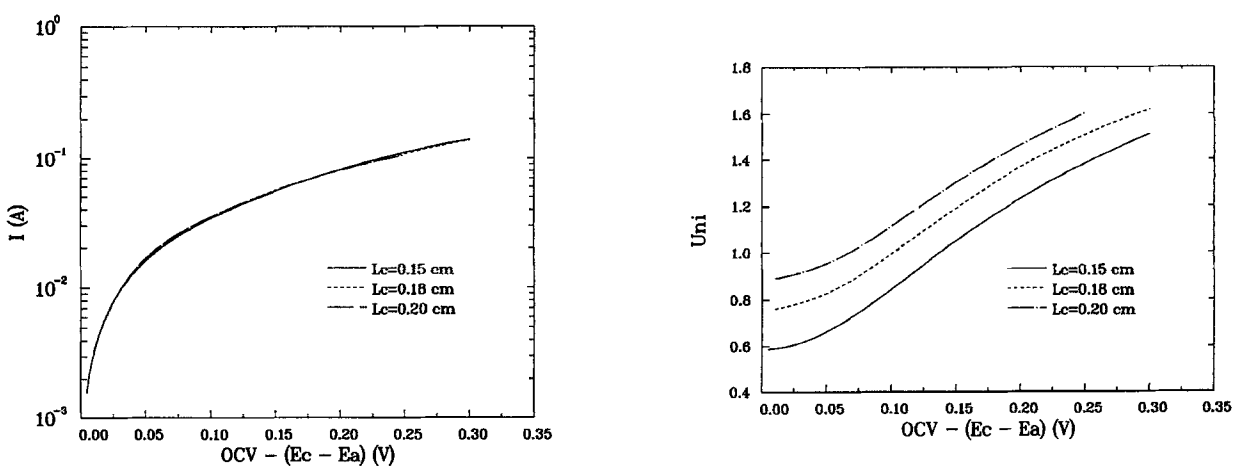

Fig. 4. The predicted effect of the cathode thickness on the discharge rate (a, left) and on the transfer current distribution (b, right). La = 0.18 cm, Ls = 0.15 cm, Lp = 0.4 cm, r = 0.12 cm.

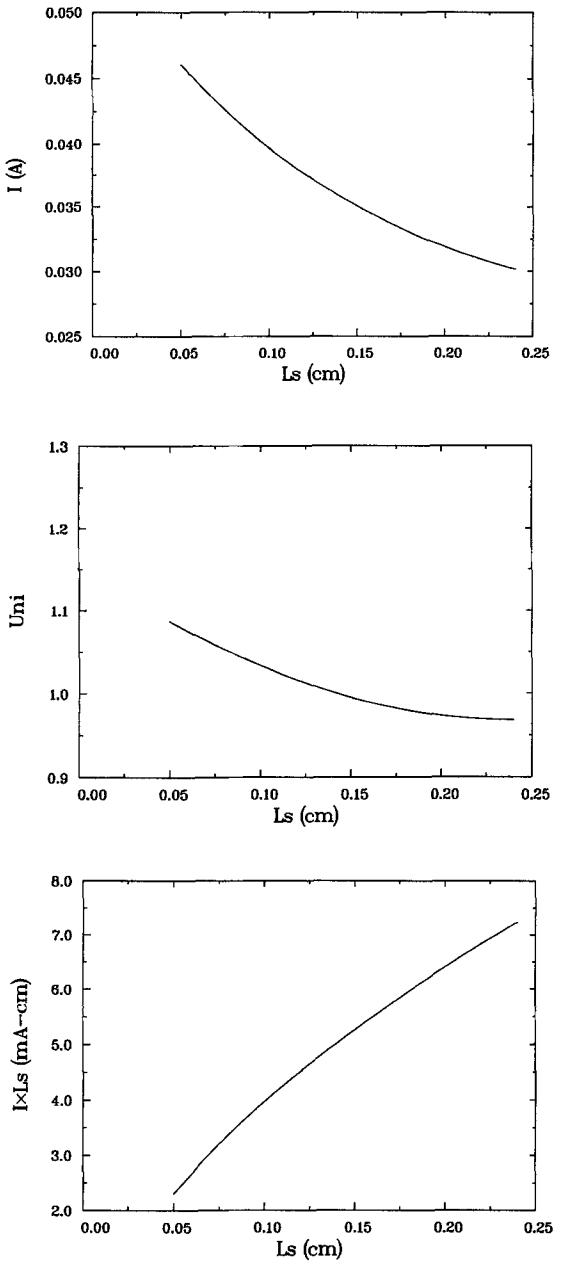

Fig. 5. The predicted effect of the separator thickness on the total current (a, top), on the transfer current distribution (b, middle), and on the product of the thickness and the current (c, bottom). Lc = 0.18 cm, La = 0.18 cm, Lp = 0.4 cm, r = 0.12 cm, OCV − (E_c − E_a) = 0.1 V.

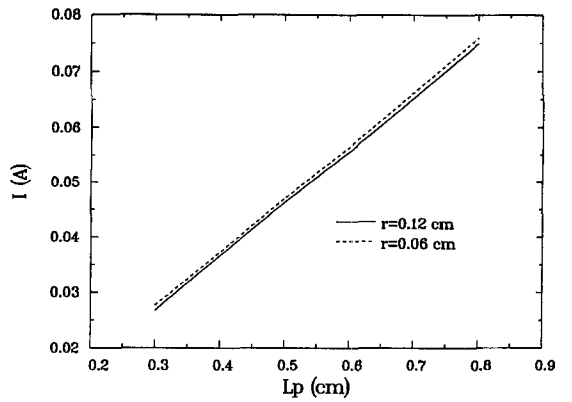

Fig. 6. The predicted dependence of discharge rate on the distance between two neighboring grid wires and the wire size. Lc = 0.18 cm, La = 0.18 cm, Ls = 0.15 cm, r = 0.12 cm, OCV − (E_c − E_a) = 0.1 V.

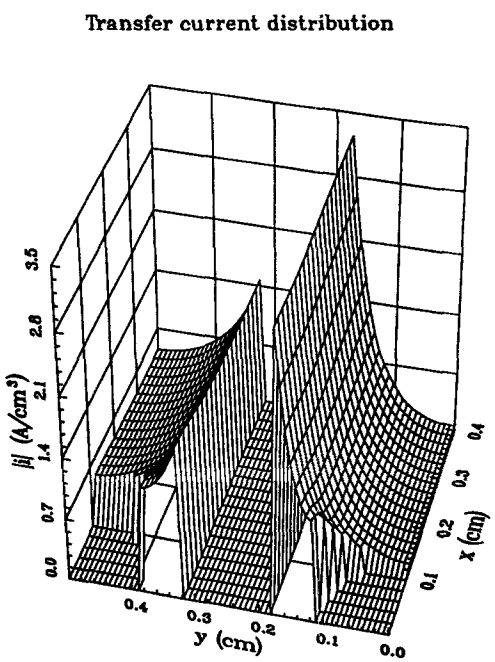

Fig. 7. A transfer current distribution when the kinetics of the reactions at the anode and the cathode are much different. L_a = 0.18 cm, L_c = 0.18 cm, Ls = 0.15 cm, Lp = 0.4 cm, r = 0.12 cm, OCV − (E_c − E_a) = 0.1 V, $i_{a,o}$ = 3.404 × 10^{-3} A/cm², $i_{c,o}$ = 2.849 × 10^{-2} A/cm².

the effect of the wire radius on the total current is insignificant. Therefore, selection of the grid wire size may be based on strength or other nonelectrical requirements.

The effect of electrode reaction kinetics on the transfer current distribution has been investigated by adjusting the exchange current densities for the anodic and the cathodic reactions. It was found that the transfer current distribution is sensitive to the electrode reaction kinetics. It can be inferred, therefore, that active material utilization and electrode rechargeability are strongly influenced by electrode design and that such design must take into account the kinetics of the electrode reactions. Figure 7 shows results from a case in which the reaction rate constant (the exchange current density for an electrochemical reaction) for the cathodic reaction is about one order of magnitude greater than that for the anodic reaction. As seen in Fig. 7, the cathodic reaction occurs predominantly on the front side of the electrode, indicating that discharge capacity of this electrode would be severely limited when the front side of the electrode is blocked by reaction product. However, both rechargeability and utilization could be improved significantly by designing the electrode to more evenly distribute the reaction products produced during such high-rate use.

Acknowledgments

The authors are grateful for the support of this work by Electrosource, Incorporated.

Manuscript submitted Sept. 10, 1990; revised manuscript received Dec. 7, 1990.

Texas A&M University assisted in meeting the publication costs of this article.

LIST OF SYMBOLS

a_a	specific surface area per unit volume of the anode, cm²/cm³
a_c	specific surface area per unit volume of the cathode, cm²/cm³
E_a	anode potential in the solid phase, V
E_c	cathode potential in the solid phase, V
$E_{a,o}$	open-circuit potential of the anode with respect to a reference electrode, V
$E_{c,o}$	open-circuit potential of the cathode with respect to a reference electrode, V
F	Faraday's constant, 96,487 C/mol

$\mathbf{i}$ unit vector in the x direction
i_a anodic current density due to the reaction at the anode, A/cm^2
i_c cathodic current density due to the reaction at the cathode, A/cm^2
I total current, A
I_f total current along front side of the cathode, A
I_b total current along the center of the cathode, A
I_{xy} current density at (x, y)
$\mathbf{j}$ unit vector in the y direction
La half thickness of the anode, cm
Lc half thickness of the cathode, cm
Ls thickness of the separator, cm
Lp half distance between the centers of two neighboring wires, cm
OCV open-circuit cell voltage, V
R universal gas constant, 8.314 J/mol-K
r radius of the grid wire, cm

Greek letters

α_a anodic transfer coefficient for the reaction at the anode
α_c cathodic transfer coefficient for the reaction at the anode
β_a anodic transfer coefficient for the reaction at the cathode
β_c cathodic transfer coefficient for the reaction at the cathode
ϵ_a porosity of the anode
ϵ_s porosity of the separator
ϵ_c porosity of the cathode
σ electrolyte conductivity, S/cm
σ_a effective electrolyte conductivity in the anode, S/cm
σ_c effective electrolyte conductivity in the cathode, S/cm
σ_s effective electrolyte conductivity in the separator, S/cm
ϕ potential in the electrolyte, V

REFERENCES

1. B. E. Jay, C. Morris, and A. Datta, Proceedings of the Fourth Annual Battery Conference on Applications and Advances, University of California, Long Beach (1989).
2. W. G. Sunu, "Electrochemical Cell Design," R. E. White, Editor, p. 357, Plenum Press, New York (1984).
3. H. Gu, T. V. Nguyen, and R. E. White, *This Journal*, **134,** 2953 (1987).
4. W. H. Tiedemann and J. Newman, in "Battery Design and Optimization," S. Gross, Editor, p. 23, The Electrochemical Society Softbound Proceedings Series, PV 79-1, Princeton, New Jersey (1979).
5. W. H. Tiedemann and J. Newman, *ibid.*, p. 39.
6. W. H. Tiedemann, J. Newman, and F. De Sua, *J. Power Sources*, **6,** 15 (1977).
7. W. G. Sunu and B. W. Burrows, *This Journal*, **129,** 688 (1982).
8. W. G. Sunu and B. W. Burrows, *ibid.*, **131,** 1 (1984).
9. E. C. Dimpault-Darcy, T. V. Nguyen, and R. E. White, *ibid.*, **135,** 278 (1988).
10. PDE/PROTRAN, A System for the Solution of Partial Differential Equations, IMSL, Inc. (1989).
11. J. Newman and W. H. Tiedemann, *AIChE J.*, **21,** 25 (1975).
12. C. F. Gerald and P. O. Wheatley, "Applied Numerical Analysis," p. 248, Addison-Wesley Publishing Company, Reading, MA (1984).
13. H. Bode, "Lead-Acid Batteries," John Wiley and Sons, New York (1977).

Current Distributions on Recessed Electrodes

Alan C. West*,[1] **and John Newman***

Materials Sciences Division, Lawrence Berkeley Laboratory, and Department of Chemical Engineering, University of California, Berkeley, California 94720

ABSTRACT

The primary current distributions on disk electrodes and two-dimensional electrodes that are recessed in insulating planes are given. The ohmic resistances are also given and are compared to previous estimates that were given in Ref. (2-5). A singular-perturbation analysis, valid for small aspect ratios, shows general behavior to be expected for all cells containing an electrode that is recessed slightly from the insulating plane.

The primary current distributions and ohmic resistances of recessed, disk, and two-dimensional electrodes are given. Recessed planar electrodes may be important, for example, for electroplating processes in the electronics industry. Recessed disk electrodes (see Fig. 1) may be designed to attain a fairly uniform current distribution on the disk (1). They are also undoubtedly used because of an inability to construct disks that are perfectly coplanar with the insulating plane.

The primary current distribution is valid when concentration variations are negligible and when the resistance of the interfacial reaction is zero. For these conditions, the distribution of current density and potential is given by Laplace's equation. The boundary conditions for the disk geometry are

$$\Phi = 0 \quad \text{as} \quad z^2 + r^2 \to \infty \qquad [1]$$

$$\Phi = V \quad \text{at} \quad z = 0 \quad \text{and} \quad r < r_o \qquad [2]$$

$$\frac{\partial \Phi}{\partial z} = 0 \quad \text{at} \quad z = L \quad \text{and} \quad r > r_o \qquad [3]$$

and

$$\frac{\partial \Phi}{\partial r} = 0 \quad \text{at} \quad r = r_o \quad \text{and} \quad 0 < z < L \qquad [4]$$

The outer radius of the insulating plane (at $z = L$) is assumed to be much larger than r_o.

Previous Work

As early as 1904, Maxwell (2) gave an approximate analysis that determined the ohmic resistance of a recessed disk electrode. He was unconcerned with the current distribution. Rayleigh (3) gave an approximate analysis, which resulted in an estimate of the mathematical equivalent to the ohmic resistance. In 1963, Kelman (4, 5) investigated a steady-state diffusion problem that is the mathematical equivalent to the ohmic resistance.

The ohmic resistance R for current flow from the recessed disk to a counterelectrode at infinity can be given by

$$R\kappa r_o = \frac{1}{4} + \frac{L}{\pi r_o} + h_a(L/r_o) \qquad [5]$$

The first two terms are the resistance of an isolated disk and the resistance of a circular cylinder. $h_a(L/r_o)$ is the ex-

* Electrochemical Society Active Member.
[1] Present address: Département des matériaux, Laboratoire de métallurgie chimique, Ecole Polytechnique Fédérale de Lausanne, MX-C Ecublens, CH-1015 Lausanne, Switzerland.